Biochemical and Biophysical Research Communications 381 (2009) 33–38

Contents lists available at ScienceDirect

Biochemical and Biophysical Research Communications

journal homepage: www.elsevier.com/locate/ybbrc

Single molecule tracking of quantum dot-labeled mRNAs in a cell nucleus

Yo Ishihama [a,b], Takashi Funatsu [a,b,c,*]

[a] Laboratory of Bio-Analytical Chemistry, Graduate School of Pharmaceutical Sciences, The University of Tokyo, 7-3-1 Hongo, Bunkyo-ku, Tokyo 113-0033, Japan
[b] Center for NanoBio Integration, The University of Tokyo, 7-3-1 Hongo, Bunkyo-ku, Tokyo 113-8656, Japan
[c] CREST, Japan Science and Technology Agency, 5 Sanbancho, Chiyoda-ku, Tokyo 102-0075, Japan

ARTICLE INFO

Article history:
Received 19 January 2009
Available online 8 February 2009

Keywords:
Single particle tracking
mRNA
Anomalous diffusion
Quantum dots

ABSTRACT

Single particle tracking (SPT) is a powerful technique for studying mRNA dynamics in cells. Although SPT of mRNA has been performed by labeling mRNA with fluorescent dyes or proteins, observation of mRNA for long durations with high temporal resolution has been difficult due to weak fluorescence and rapid photobleaching. Using quantum dots (QDs), we succeeded in observing the movement of individual mRNAs for more than 60 s, with a temporal resolution of 30 ms. Intronless and truncated *ftz* mRNA, synthesized *in vitro* and labeled with QDs, was microinjected into the nuclei of Cos7 cells. Almost all mRNAs were in motion, and statistical analyses revealed anomalous diffusion between barriers, with a microscopic diffusion coefficient of 0.12 $\mu m^2/s$ and a macroscopic diffusion coefficient of 0.025 $\mu m^2/s$. Diffusion of mRNA was observed in interchromatin regions but not in histone2B-GFP-labeled chromatin regions. These results provide direct evidence of channeled mRNA diffusion in interchromatin regions.

mRNAs are transcribed and processed in the nucleus and are then exported to the cytoplasm for translation. mRNA export from the nucleus to the cytoplasm is a highly selective process, and is important for the regulation of gene expression of eukaryotic cells [1]. The mechanism of mRNA movement from the site of transcription to the nuclear pore has been extensively studied [2–9]. Politz et al. labeled endogenous poly(A)$^+$ RNAs with fluorescent oligo(dT) and measured their intranuclear movement by fluorescence correlation spectroscopy and fluorescence recovery after photobleaching (FRAP). They reported that about 1/3 of poly(A)$^+$ RNAs were randomly moving with a diffusion constant, $D = 0.6\ \mu m^2/s$ or slower, and that the other 2/3 s were moving more rapidly with $D = 9\ \mu m^2/s$, which was comparable to the movement of poly(A)$^+$ RNA in water [3]. They also measured D of poly(A)$^+$ RNAs using caged fluorescein-conjugated oligo(dT) and spot-illuminated photolysis for uncaging. These studies showed that poly(A)$^+$ RNAs diffused with $D = 0.6\ \mu m^2/s$ [4]. These studies were based on hybridization of antisense oligo DNA probes to RNA, however, it is now accepted that hybrid of DNA-RNA is not stable *in vivo*. Molenaar et al. used a 2′*O*-methyl oligo(U)$_{22}$ probe to improve the stability of the hybrid and found by FRAP analysis that poly(A)$^+$ RNAs were moving with $D = 0.04\ \mu m^2/s$ [2]. This result suggested that what Politz et al. observed was not diffusion of poly(A)$^+$ RNA. However, the possibility remains that the difference in D was due to different observation conditions. For instance, D of a receptor protein in a cell membrane is known to be different depending on observation conditions, such as time resolution and observation area because of non-homogeneity of the cell membrane [10].

SPT is expected to resolve this issue because it enables us to analyze the movement of individual RNA molecules in real time and to compare the relationship between movement and the subnuclear structure. Recently, SPT of mRNA visualized by the MS2-GFP (green fluorescent protein) system was performed in the nucleus [6] and in the cytoplasm [11]. In the MS2-GFP system, a MS2 tag sequence is introduced into the target mRNA and it is labeled by a fusion protein of MS2 and GFP. Shav-Tal et al. reported that half the population of mRNAs diffused freely, with $D = 0.04–0.05\ \mu m^2/s$, and the other half were in corralled motion in the nucleus [6]. SPT of mRNA labeled with a molecular beacon (MB) was performed in the nucleus [8]. A MB is a hairpin-shaped oligonucleotide that contains a fluorophore and a quencher at the 5′ and 3′ ends, respectively, and emits fluorescence upon hybridization to the complementary sequence of mRNA. Brownian motion of mRNA with $D = 0.03\ \mu m^2/s$ was reported [8]. However, these two studies were carried out with low temporal resolution (300 ms/frame) and mRNAs were only observed over 3 s. Thus the possibility remains that mRNAs moving rapidly due to diffusion were not captured. Tadakuma et al. microinjected fluorescently labeled mRNAs to the nucleus and observed by confocal microscopy them every 30 ms. They determined a faster $D = 0.2\ \mu m^2/s$ [7]. Although this study showed that mRNA moves rapidly over a short time range, the observation duration was limited to 1 s because mRNA molecules departed from the confocal plane.

* Corresponding author. Address: Laboratory of Bio-Analytical Chemistry, Graduate School of Pharmaceutical Sciences, The University of Tokyo, 7-3-1 Hongo, Bunkyo-ku, Tokyo 113-0033, Japan. Fax: +81 3 5802 3339.
E-mail address: funatsu@mail.ecc.u-tokyo.ac.jp (T. Funatsu).

0006-291X/$ - see front matter © 2009 Elsevier Inc. All rights reserved.
doi:10.1016/j.bbrc.2009.02.001

In this study, we tried to analyze the movement of mRNA every 30 ms over a duration of about 60 s using quantum dots (QDs) because QDs emit intense fluorescence and are resistant to photobleaching [12,13]. QDs were attached to mRNAs in a stoichiometric ratio of 1:1 and SPT was performed by epifluorescence microscopy. We succeeded in performing SPT of mRNA-QDs in living cell nuclei and we compared SPT in the interchromatin region with that in the chromatin region.

Materials and methods

Cell cultures. Cos7 cells were cultured in a medium consisting of Dulbecco's modified Eagle's medium supplemented with 10% fetal calf serum at 37 °C in 5% CO_2. The cells were sub-cultured in a medium without phenol red (#21063-029; Invitrogen Japan, Tokyo, Japan) in glass-bottom culture dishes (#3910-035; Asahi Techno Glass, Tokyo, Japan) for 1–2 days before mRNA injection.

Preparation of oligo(U)$_{22}$-QD. 2′*O*-methyl oligo(U)$_{22}$, whose 3′ end contained a thiol group, was synthesized by Sigma Genosys (Ishikari, Japan) as a 22 mer. Conjugation of amino-modified QDs (ITK amino PEG QD565; Invitrogen) to oligo(U)$_{22}$ was performed according to Derfus et al. [14]. NHS-PEG4-Maleimide (Pierce, IL) was used to cross-link QD and oligo(U)$_{22}$, and Methyl-PEG4-NHS (Pierce) was used to control the efficiency of conjugation. A 1000-fold excess of a mixture of NHS-PEG4-Maleimide and Methyl-PEG4-NHS was reacted with QDs for 1 h in 50 mM sodium phosphate and 150 mM sodium chloride (pH 7.2). Free NHS-PEG4-Maleimide and Methyl-PEG4-NHS were removed from QDs with a NAP-5 column (GE Healthcare, NJ). Thiol-containing oligo(U)$_{22}$ was reduced with 40 mM dithiothreitol (DTT) for 16 h and then filtered with a NAP-5 column to remove DTT. QDs and oligo(U)$_{22}$ were then cross-linked in 50 mM sodium phosphate, 150 mM sodium chloride, and 10 mM EDTA for 6 h. After the reaction, unreacted maleimide was quenched by incubation with 0.1 mM 2-mercaptoethanol for 30 min. To remove free oligo(U)$_{22}$, QDs were washed with PBS buffer and 3× SSC buffer (45 mM sodium citrate and 450 mM sodium chloride) using Amicon Ultra-4 filters (cutoff molecular weight is 100 kDa). QDs labeled with oligo(U)$_{22}$ in a 1:1 ratio were purified with Dynabeads MyOne Streptavidin C1 (Invitrogen) and biotinylated oligo DNA (A)$_{25}$ (Operon Biotechnologies, Tokyo, Japan). Finally, oligo(U)$_{22}$-QDs were suspended in 10 mM Tris–HCl (pH 7.5).

Microinjection. To prepare truncated, mature, intron-less *ftz* mRNAs, pGEM mature-ftz (kindly donated by Mutsuhito Ohno, Kyoto University) was amplified by PCR. For *in vitro* transcription, the PCR-amplified mature *ftz* DNAs were transcribed using a RiboMAX kit (P2180; Promega K.K., Japan, Tokyo, Japan). A cap analog, m^7GpppG (P1812; Promega), was incorporated into the 5′ end of the mRNAs during the transcription reaction (the ratio of cap analog:GTP in the reaction mixture was 5:1). Oligo(U)$_{22}$–QD and mature *ftz* mRNAs containing poly(A)$_{40}$ were incubated in PBS buffer with final concentrations of 2 μM mRNAs and 5 nM QDs for 10 min. Microinjection of the solution into the nuclei of Cos7 cells was performed using an injector (FemtoJet + Micromanipulator 5171; Eppendorf Japan, Tokyo, Japan) equipped with a microneedle (Femtotips II; Eppendorf). The injection duration was 0.2 s, and the injection and compensation pressures were 15 hPa.

Single particle tracking of mRNA-QDs. QD-labeled mature *ftz* mRNAs (termed mRNA-QDs) were observed using an epi-fluorescence microscope (IX-70; Olympus, Tokyo, Japan) equipped with a cooled EM-CCD camera (iXon^{EM}+; Andor Technology, Belfast, Northern Ireland) and an oil-immersion objective (PlanApo 60×, NA = 1.4; Olympus). QDs were excited with a blue solid-state laser (488 nm, Sapphire 488-30; Coherent Japan, Tokyo, Japan). A dichroic mirror, Q505LP, (Chroma, Rockingham, VT) and an emission filter, HQ565/20M, (Chroma) were used for QD imaging. Temperatures of the sample and objective lens were kept at 37 °C by a thermo plate (INUG2-ONI, Tokai Hit, Fujinomiya, Japan) and a lens heater (MATS-LH, Tokai Hit), respectively. QDs alone or mRNA-QDs were tracked every 30 ms with a tracking program (Aquacosmos software; Hamamatsu Photonics, Hamamatsu, Japan). A QD with a mean square displacement (MSD) for 10 s of less than 0.1 μm^2 was regarded as stationary and the data were excluded from the analysis (0.67% of QDs and 0.52% of mRNA-QDs were defined as stationary). The ensemble averaged MSD of QDs or of RNA-QDs was calculated with Eq. (1);

$$\mathrm{MSD} = < dx^2 + dy^2 >, \tag{1}$$

where dx and dy represent displacement at x and y axes, respectively. The MSD-t plot of simple diffusion was fitted with Eq. (2);

$$\mathrm{MSD} = 4Dt, \tag{2}$$

where the parameter D is the diffusion coefficient of simple diffusion and t is time interval. The MSD-t plot of diffusion with barriers was fitted with Eq. (3) [15–17];

$$\mathrm{MSD} = \frac{L^2}{3}\left(1 - e^{-\frac{t}{\tau}}\right) + 4D_{MACRO}t \tag{3}$$

where D_{MACRO} is the macroscopic diffusion coefficient, L is the size of a micro-compartment, and τ is equilibration time. D_{micro}, the microscopic diffusion coefficient, was obtained from Eq. (4).

$$D_{micro} = \frac{L^2}{12\tau} \tag{4}$$

To compare the diffusion of QDs and mRNA-QDs in solution, they were diluted in PBS buffer containing 50% sucrose and their fluorescent images were taken at 23 °C and analyzed as described. *D*s in solution at 37 °C were calculated assuming that the viscosity of PBS buffer is 0.69 mPa s at 37 °C and that of 50% sucrose solution is 14.6 mPa s at 2 °C.

Comparison of mRNA movement in the interchromatin region with the chromatin region. Cos7 cells were transfected with H2BGFP-N1 plasmid [18] (kindly donated by Teru Kanda, Hokkaido University) using Fugene 6 transfection reagent (Roche Diagnostics K.K., Tokyo, Japan) and cultured for 18–24 h before use. Chromatin labeled with H2B-GFP, and mRNA-QDs were observed with a Nipkow disk-type confocal unit (CSU-10; Yokogawa Electric, Tokyo, Japan) and an oil-immersion objective (PlanApo 150x, NA = 1.45; Olympus). Both GFP and QDs were excited with a blue solid-state laser (Sapphire 488-20; Coherent Japan). Emission filters for GFP and QDs were EF01-520/35-25 (Semrock, Rochester, NY) and HQ565/20M, respectively. Fluorescence images were captured with an EM-CCD camera (C9100-12; Hamamatsu Photonics, Hamamatsu, Japan). Chromatin labeled with H2B-GFP and trajectories of QDs were superimposed. The SPT of QDs and of mRNA-QDs was used to calculate the ratios of the residence time per unit area of interchromatin region to that in the chromatin region. We analyzed an interchromatin area of 49.8 μm^2 for QDs and 16.9 μm^2 for mRNA-QDs, and a chromatin area of 57.9 μm^2 for QDs and 14.4 μm^2 for mRNA-QDs.

Results and discussion

Stoichiometric 1:1 labeling of mRNA with QDs

To label the 3′ poly(A) tail of mRNAs with oligo(U)$_{22}$-QDs, amino-modified QDs and oligo(U)$_{22}$, which contained a thiol group at the 3′ end, were cross-linked with NHS-PEG-maleimide. As a QD contains many amino groups, we used NHS-PEG-methyl as a competitor of NHS-PEG-maleimide to control the labeling ratio. We

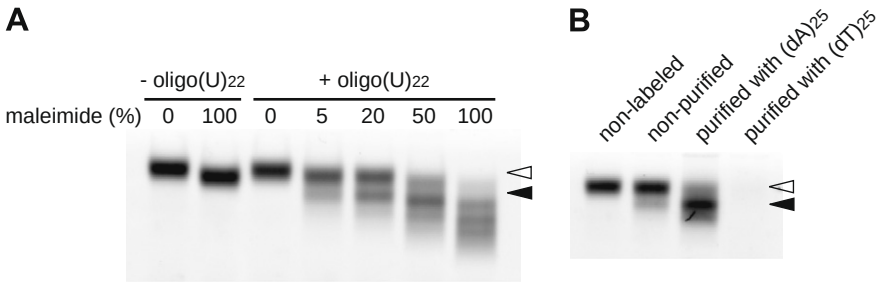

Fig. 1. Preparation of QD-labeled 2′*O*-methyl oligo(U)$_{22}$. (A) 2′*O*-methyl oligo(U)$_{22}$ and QD were cross-linked with various ratios of NHS-PEG4-Maleimide and Methyl-PEG4-NHS, and analyzed by 1% agarose gel electrophoresis. (B) Purification of Oligo(U)$_{22}$-QD. QD was conjugated with oligo(U)$_{22}$ in the presence of 5% NHS-PEG-Maleimide, and unconjugated QDs were removed by purification with (dA)$_{25}$-magnetic microspheres. Purification using (dT)$_{25}$ was performed as a negative control. Open arrowheads indicate unconjugated QDs and closed arrowheads indicate oligo(U)$_{22}$ and QD conjugated in a 1:1 ratio.

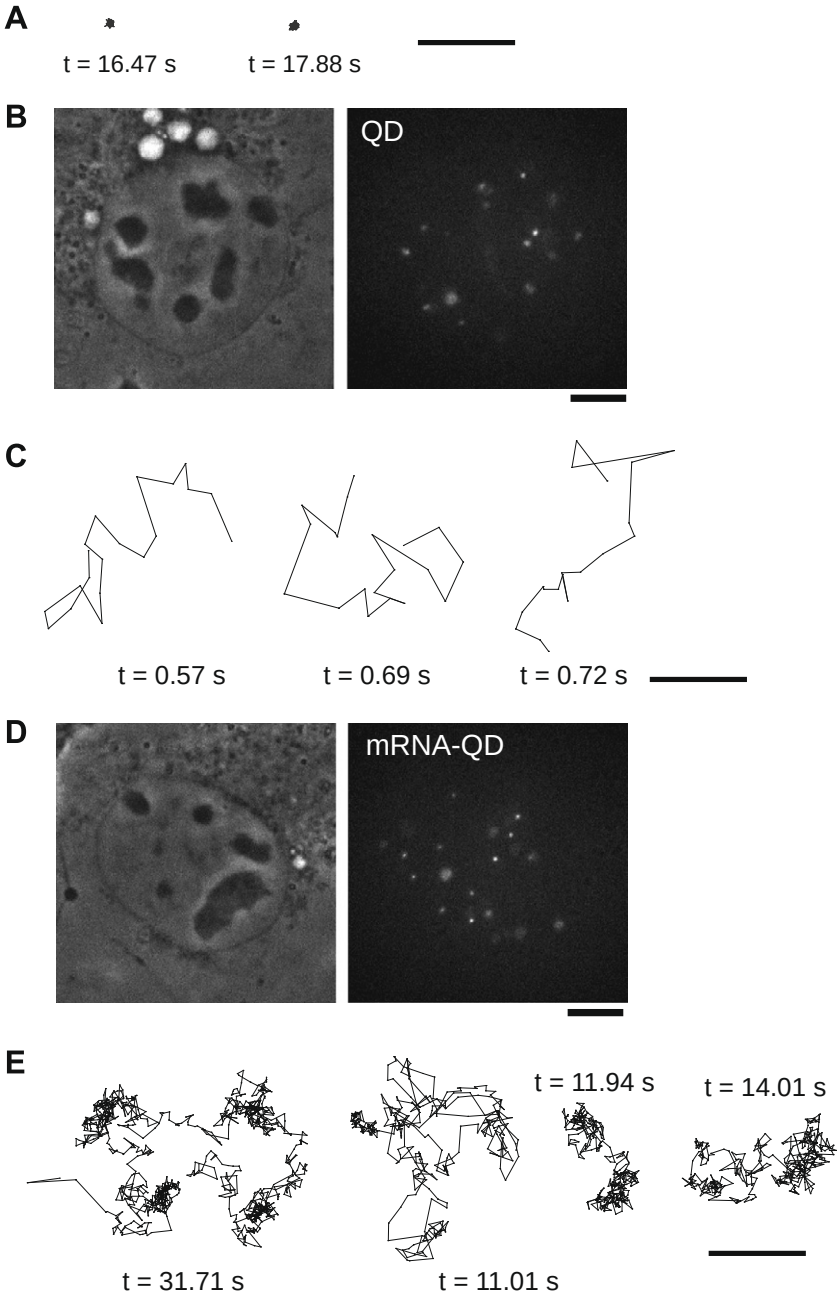

Fig. 2. Fluorescence micrographs and SPT of QDs and of mRNA-QDs in the nucleus of Cos7 cells. (A) Trajectories of QDs immobilized on a glass surface. Times indicate observation durations. Scale bars in (A,C,E), 1 μm. (B) Phase-contrast and fluorescence micrographs of a nucleus injected with QDs. Scale bars in (B,D), 10 μm. (C) Typical trajectories of QDs in a nucleus. (D) Phase-contrast and fluorescence micrographs of a nucleus injected with mRNA-QDs. (E) Typical trajectories of mRNA-QDs.

confirmed conjugation of oligo$(U)_{22}$ to QD by agarose gel electrophoresis (Fig. 1A). Compared with unconjugated QDs, oligo$(U)_{22}$-QDs showed increasing gel shift with increased NHS-PEG-maleimide ratios. We evaluated that the labeling ratio of oligo$(U)_{22}$ to QD was 40% when NHS-PEG-Maleimide was mixed with NHS-PEG-methyl at a molar ratio of 5:95, which was confirmed using Cy5-labeled 2′*O*-methyl oligo$(U)_{22}$ (data not shown). Oligo$(U)_{22}$-QDs were purified using poly$(A)_{25}$ DNA conjugated magnetic beads to remove non-labeled QDs. The purified product was a 1:1 stoichiometric complex of Oligo$(U)_{22}$ and QD (Fig. 1B).

Single particle tracking of QDs and mRNA-QDs

QD labeling allowed mRNAs to be observed with high temporal and spatial resolution over long observation durations, which have not been achieved by conventional labeling with a fluorescent dye or fluorescent protein. First, we evaluated the spatial resolution for SPT of QDs. Fluorescence images of QDs adsorbed on a glass surface were captured every 30 ms for about 16 s and the positions were determined with two dimensional Gaussian fitting (Fig. 2A). The standard deviation was 20 nm. Prior to tracking mRNA-QDs in the nucleus, SPT of QDs was performed. QDs were microinjected into the nucleus of living Cos7 cells and their movements were observed (Fig. 2B and C). Microinjected QDs were diffusely distributed in the nucleoplasm except for in the nucleoli. QDs were observed moving freely with little adsorption to the nuclear structure (Fig. 2C). Next, mRNA-QDs were microinjected into the nucleus of living Cos7 cells. mRNA-QDs were observed every 30 ms for about 30 s and were seen as fluorescent spots in the nucleus (Fig. 2D and E). Individual fluorescent spots appeared with homogeneous fluorescence intensity and characteristic blinking (data not shown) and were judged to be single QDs. mRNA-QDs appeared to be in Brownian motion in compartmentalized areas, however they were sometimes observed to jump to other compartmentalized areas (Fig. 2E). The motion of mRNA-QDs was similar to hop diffusion of some receptors in the cell membrane [10,15].

Movement of QDs and mRNA-QDs in a solution and in the nucleus were statistically analyzed. First, to reduce their mobility, QDs was observed in a 50% sucrose solution at 23 °C. An MSD-*t* plot showed that MSD increased linearly with time and that it could be fitted with Eq. (1) (Fig. 3A). From the slope of the MSD-*t* plot, *D* was determined to be 0.87 $\mu m^2/s$. The *D* value of QD in PBS solution at 37 °C was calculated to be 18.4 $\mu m^2/s$. The MSD of mRNA-QDs in a 50% sucrose solution at 23 °C also increased linearly with time (Fig. 3A) and $D = 0.57\ \mu m^2/s$. The *D* value of mRNA-QD in PBS solution at 37 °C was deduced to be 12.1 $\mu m^2/s$. The MSD of QDs in the nucleus at 37 °C also increased linearly with time and could be fitted with Eq. (1) (Fig. 3B). This result indicated that QDs were in free diffusion in the nucleus with $D = 1.42\ \mu m^2/s$. The *D* value of QDs in the nucleus was about 1/13 of that in PBS solution. This was smaller than the values determined for GFP or dextran (1/3–1/5 of the value in PBS) [19,20], presumably due to the larger size of QDs.

On the other hand, the MSD of mRNA-QDs in the nucleus did not increase linearly (Fig. 3B). This result indicated that the movement of mRNA-QDs in the nucleus was anomalous diffusion [21–23]. Although anomalous diffusion of receptor proteins in the cell membrane [10,15], in chromatin [17,24] and in subnuclear domains [25,26] has been reported, anomalous diffusion of mRNA has not been intensively studied. This MSD-*t* plot was well fitted with Eq. (2), which was derived assuming confined diffusion within a barrier over a short time range and hop diffusion between barriers over a long time range [15–17]. The size of the barrier is characterized by *L*. Diffusion within barriers and hop diffusion between barriers are characterized by D_{micro} and D_{MACRO}, respectively. These parameters were determined by fitting the data with Eq. (2) as follows: $L = 0.97\ \mu m$, $D_{micro} = 0.12\ \mu m^2/s$, $D_{MACRO} = 0.025\ \mu m^2/s$. D_{micro} and D_{MACRO} were about 1/100 and 1/490 of *D* in PBS solution, respectively. This result suggests interaction of mRNA with the intranuclear structure, presumably involving rapid association and dissociation from the structure. These results are consistent with previous reports of mRNA diffusion in the nucleus, i.e., D_{micro} was similar to *D* measured over a short time range [7] and D_{MACRO} was comparable to *D* over a long time range [2,6,8]. The differences in *D* values reported previously may be partly due to differences in observation conditions, such as temporal resolution and observation duration.

Comparison of mRNA-QD movement in the interchromatin region with movement in the chromatin region

The anomalous diffusion of mRNA-QDs is likely to be due to Brownian motion of mRNAs within an intranuclear structure. A candidate for such a structure is chromatin [27]. To compare the interchromatin region with the chromatin region, chromatin was visualized with H2B-GFP [18]. Cos7 cells expressing H2B-GFP were observed by confocal microscopy and the chromatin structure was examined (Fig. 4). First, QDs were injected into the nucleus of a cell expressing H2B-GFP and QD movements were analyzed. Trajectories of QDs were superimposed onto chromatin regions (Fig. 4A). QDs were diffusely distributed in all nucleoplasmic regions, except

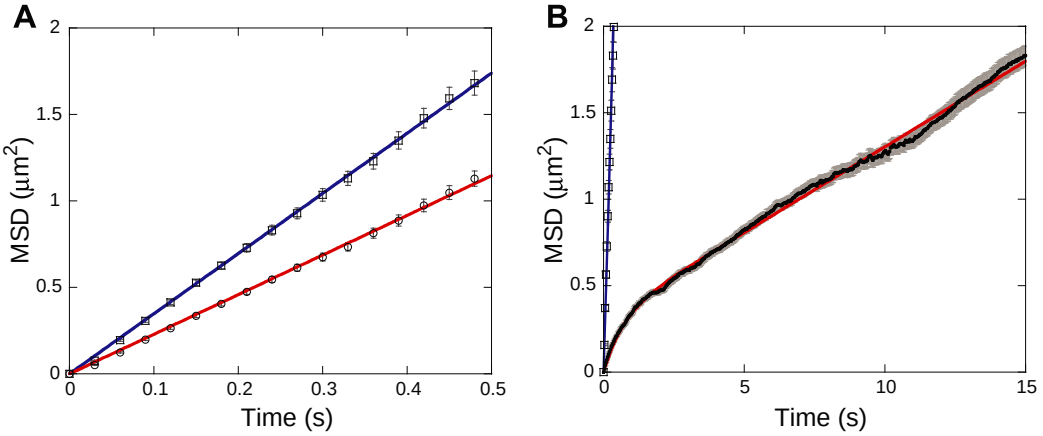

Fig. 3. MSD-*t* plot of QDs and mRNA-QDs. (A) MSD-*t* plot of QDs and mRNA-QDs in 50% sucrose solutions. Squares indicate QDs ($n = 280$) and circles indicate mRNA-QDs ($n = 316$). Error bars indicate standard errors of the mean. Fitting lines were obtained using Eq. (1). (B) MSD-*t* plot of QDs and mRNA-QDs in the nuclei of Cos7 cells. Squares indicate QDs (4 cells; $n = 296$) and small dots indicate mRNA-QDs (7 cells; $n = 384$). The fitting lines of QDs (blue) and mRNA-QDs (red) were obtained using Eqs. (1) and (2), respectively.

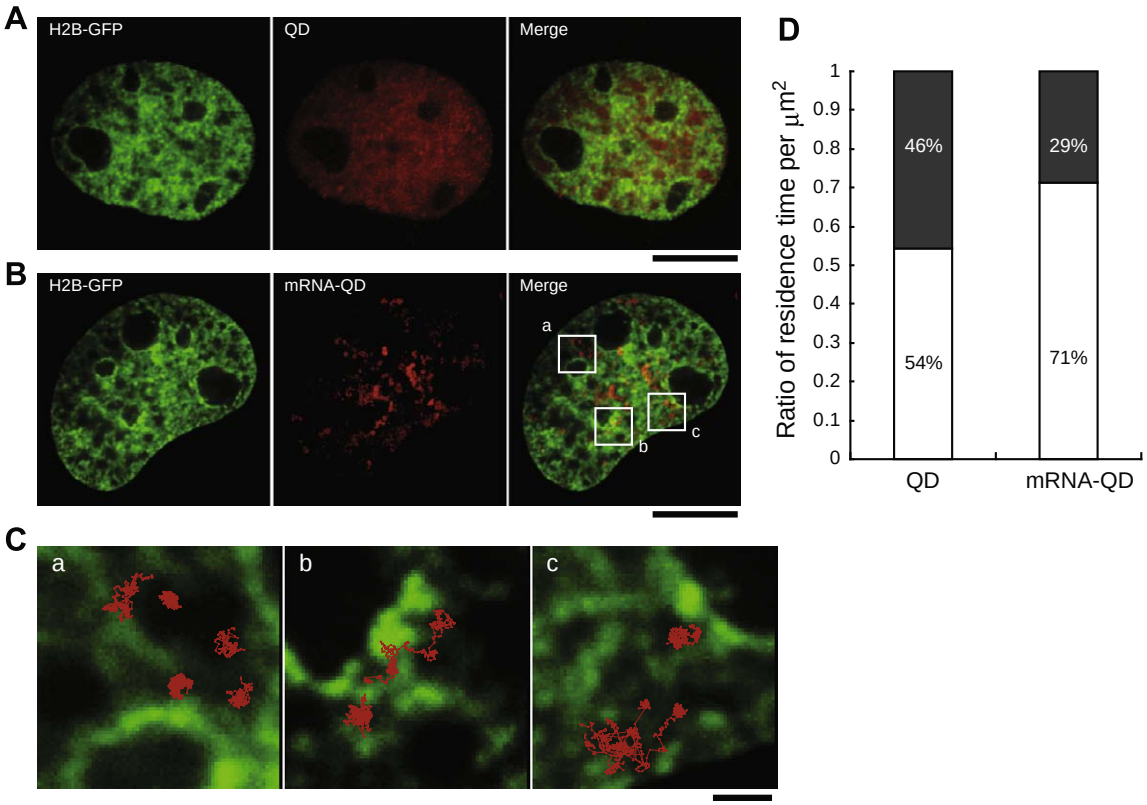

Fig. 4. Comparison of mRNA-QD movement in the interchromatin region with movement in the chromatin region. Chromatin regions were visualized with H2B-GFP. (A) QDs were injected into the nuclei of Cos7 cells expressing H2B-GFP and the localization of QDs and chromatin were compared. Scale bar, 10 μm. (B) mRNA-QDs were injected into the nucleus of Cos7 cells expressing H2B-GFP. Trajectories of mRNA-QDs were compared with chromatin regions. Scale bar, 10 μm. (C) Magnified views of the areas a, b, and c in (B). Scale bar, 1 μm. (D) The ratio of residence time per μm^2 in the interchromatin region (white bars) to that in the chromatin region (black bars) were determined by SPT of QDs and mRNA-QDs. 39 mRNA-QDs and 159 QDs were analyzed.

nucleoli, indicating that the chromatin domain was not an obstacle to the Brownian motion of QDs. Next, mRNA-QDs were injected into the nucleus of a cell expressing H2B-GFP and the mRNA-QD movements were analyzed. All mRNA-QDs observed for 90 s were traced and their trajectories were compared with the interchromatin regions (Fig. 4B and C). The trajectories of mRNA-QDs scarcely occurred in chromatin regions, indicating that mRNA-QDs spent more than 70% of the time in the interchromatin space (Fig. 4C and D). These results support the hypothesis of channel diffusion of pre-mRNAs [9], endogenous poly(A)$^+$ mRNAs [4] and mRNP complexes [8]. However, mRNA-QDs provided more information compared with that obtained by previous studies of mRNA diffusion in the nucleus. For example, the average distance of interchromatin regions was about 1 μm and this value coincided with the restricted barrier size *L* determined from Fig. 3, suggesting that chromatin regions restricted mRNA movements. Furthermore, observation of long trajectories of single RNA molecules with high spatial and temporal resolutions revealed the stochastic changes between fast Brownian motion in interchromatin regions and confined Brownian motion in chromatin regions, which had not been determined by a previous study observing short RNA trajectories [7]. These results also resolved the discrepancy of apparently different diffusion coefficients; a fast diffusion coefficient (0.2 μm^2/s), obtained by observations over a short time range with high temporal resolution [7] and a slow diffusion coefficient (0.03–0.05 μm^2/s) obtained by observations over a long time range with low temporal resolution [2,6,8]. QD imaging with high spatial and temporal resolutions is effective in analyzing the dynamics of mRNAs in the nucleus at a single particle level.

Acknowledgments

We thank Teru Kanda for providing the H2BGFP-N1 plasmid. We thank Yoshitaka Shirasaki for MSD-*t* calculation. We also thank Hisashi Tadakuma, Mai Yamagishi, and Kohki Okabe for discussions. This work was partly supported by a Grant in Aid for Scientific Research A (to T.F.) from the Japan Society for the Promotion of Science.

References

[1] G. Dreyfuss, V.N. Kim, N. Kataoka, Messenger-RNA-binding proteins and the messages they carry, Nat. Rev. Mol. Cell. Biol. 3 (2002) 195–205.
[2] C. Molenaar, A. Abdulle, A. Gena, H.J. Tanke, R.W. Dirks, Poly(A)$^+$ RNAs roam the cell nucleus and pass through speckle domains in transcriptionally active and inactive cells, J. Cell. Biol. 165 (2004) 191–202.
[3] J.C. Politz, E.S. Browne, D.E. Wolf, T. Pederson, Intranuclear diffusion and hybridization state of oligonucleotides measured by fluorescence correlation spectroscopy in living cells, Proc. Natl. Acad. Sci. USA 95 (1998) 6043–6048.
[4] J.C. Politz, R.A. Tuft, T. Pederson, R.H. Singer, Movement of nuclear poly(A) RNA throughout the interchromatin space in living cells, Curr. Biol. 9 (1999) 285–291.
[5] J.C. Politz, R.A. Tuft, K.V. Prasanth, N. Baudendistel, K.E. Fogarty, L.M. Lifshitz, J. Langowski, D.L. Spector, T. Pederson, Rapid, diffusional shuttling of poly(A) RNA between nuclear speckles and the nucleoplasm, Mol. Biol. Cell 17 (2006) 1239–1249.
[6] Y. Shav-Tal, X. Darzacq, S.M. Shenoy, D. Fusco, S.M. Janicki, D.L. Spector, R.H. Singer, Dynamics of single mRNPs in nuclei of living cells, Science 304 (2004) 1797–1800.
[7] H. Tadakuma, Y. Ishihama, T. Shibuya, T. Tani, T. Funatsu, Imaging of single mRNA molecules moving within a living cell nucleus, Biochem. Biophys. Res. Commun. 344 (2006) 772–779.
[8] D.Y. Vargas, A. Raj, S.A. Marras, F.R. Kramer, S. Tyagi, Mechanism of mRNA transport in the nucleus, Proc. Natl. Acad. Sci. USA 102 (2005) 17008–17013.

[9] Z. Zachar, J. Kramer, I.P. Mims, P.M. Bingham, Evidence for channeled diffusion of pre-mRNAs during nuclear RNA transport in metazoans, J. Cell Biol. 121 (1993) 729–742.
[10] K. Murase, T. Fujiwara, Y. Umemura, K. Suzuki, R. Iino, H. Yamashita, M. Saito, H. Murakoshi, K. Ritchie, A. Kusumi, Ultrafine membrane compartments for molecular diffusion as revealed by single molecule techniques, Biophys. J. 86 (2004) 4075–4093.
[11] D. Fusco, N. Accornero, B. Lavoie, S.M. Shenoy, J.M. Blanchard, R.H. Singer, E. Bertrand, Single mRNA molecules demonstrate probabilistic movement in living Mammalian cells, Curr. Biol. 13 (2003) 161–167.
[12] M. Dahan, S. Levi, C. Luccardini, P. Rostaing, B. Riveau, A. Triller, Diffusion dynamics of glycine receptors revealed by single-quantum dot tracking, Science 302 (2003) 442–445.
[13] X. Michalet, F.F. Pinaud, L.A. Bentolila, J.M. Tsay, S. Doose, J.J. Li, G. Sundaresan, A.M. Wu, S.S. Gambhir, S. Weiss, Quantum dots for live cells, in vivo imaging, and diagnostics, Science 307 (2005) 538–544.
[14] A.M. Derfus, A.A. Chen, D.H. Min, E. Ruoslahti, S.N. Bhatia, Targeted quantum dot conjugates for siRNA delivery, Bioconjug. Chem. 18 (2007) 1391–1396.
[15] F. Daumas, N. Destainville, C. Millot, A. Lopez, D. Dean, L. Salome, Confined diffusion without fences of a G-protein-coupled receptor as revealed by single particle tracking, Biophys. J. 84 (2003) 356–366.
[16] N. Destainville, L. Salome, Quantification and correction of systematic errors due to detector time-averaging in single-molecule tracking experiments, Biophys. J. 90 (2006) L17–L19.
[17] V. Levi, Q. Ruan, M. Plutz, A.S. Belmont, E. Gratton, Chromatin dynamics in interphase cells revealed by tracking in a two-photon excitation microscope, Biophys. J. 89 (2005) 4275–4285.
[18] T. Kanda, K.F. Sullivan, G.M. Wahl, Histone-GFP fusion protein enables sensitive analysis of chromosome dynamics in living mammalian cells, Curr. Biol. 8 (1998) 377–385.
[19] Y. Chen, J.D. Muller, Q. Ruan, E. Gratton, Molecular brightness characterization of EGFP in vivo by fluorescence fluctuation spectroscopy, Biophys. J. 82 (2002) 133–144.
[20] O. Seksek, J. Biwersi, A.S. Verkman, Translational diffusion of macromolecule-sized solutes in cytoplasm and nucleus, J. Cell. Biol. 138 (1997) 131–142.
[21] M.J. Saxton, Anomalous diffusion due to obstacles: a Monte Carlo study, Biophys. J. 66 (1994) 394–401.
[22] M.J. Saxton, Single-particle tracking: effects of corrals, Biophys. J. 69 (1995) 389–398.
[23] M.J. Saxton, Anomalous diffusion due to binding: a Monte Carlo study, Biophys. J. 70 (1996) 1250–1262.
[24] J. Vazquez, A.S. Belmont, J.W. Sedat, Multiple regimes of constrained chromosome motion are regulated in the interphase Drosophila nucleus, Curr. Biol. 11 (2001) 1227–1239.
[25] S.M. Gorisch, M. Wachsmuth, C. Ittrich, C.P. Bacher, K. Rippe, P. Lichter, Nuclear body movement is determined by chromatin accessibility and dynamics, Proc. Natl. Acad. Sci. USA 101 (2004) 13221–13226.
[26] M. Platani, I. Goldberg, A.I. Lamond, J.R. Swedlow, Cajal body dynamics and association with chromatin are ATP-dependent, Nat. Cell. Biol. 4 (2002) 502–508.
[27] T. Cremer, C. Cremer, Chromosome territories, nuclear architecture and gene regulation in mammalian cells, Nat. Rev. Genet. 2 (2001) 292–301.